International Science and Technology Journal
المجلة الدولية للعلوم والتقنية

Volume 38 العدد
Part 1 المجلد

http://www.doi.org/10.62341/jfhc2358

Received	**2026/01/05**	**تم استلام الورقة العلمية في**
Accepted	**2026/01/24**	**تم قبول الورقة العلمية في**
Published	**2026/01/25**	**تم نشر الورقة العلمية في**

Critical Behavior of Maximum Shear Stress in an Unsteady Stagnation-Point Boundary Layer with Oscillatory Wall Blowing

Ali Mohamed Belhaj[1]

Higher Institute of Science and Technology, Zahra, Libya

Ali.belhag@yahoo.com

Hweda Muftah Sharif[2]

Technical College of Civil Aviation, Esbea, Libya

hwedasharif@gmail.com

Salim Ali Shawesh[3]

Technical College of Civil Aviation, Esbea, Libya

alshaweshsalim2@gmail.com

Abstract

This paper examines the influence of the unsteadiness parameter on the maximum wall shear stress in an unsteady stagnation-point boundary layer over a vertical flat plate with oscillatory wall blowing or suction. The analysis considers a two-dimensional, incompressible, viscous flow impinging on the plate, with time-periodic variations in both the free-stream velocity and the wall blowing/suction rate. The formulation follows the approach of Blyth and Hall.

Using similarity transformations, the time-dependent Navier–Stokes equations are reduced to a single nonlinear ordinary differential equation governing the boundary layer. This equation is solved numerically using a fully implicit finite-difference scheme. Wall shear stress is obtained from the second derivative of the similarity function, and its maximum value is tracked over time to characterize the flow dynamics.

http://www.doi.org/10.62341/jfhc2358

Results show that increasing the blowing parameter raises the peak shear stress, whereas larger unsteadiness reduces it. For each set of flow conditions, the shear stress reaches a maximum at a specific oscillation frequency before asymptotically approaching a steady-state trend. Higher unsteadiness delays the occurrence of this peak and diminishes its magnitude. In certain parameter ranges, the shear stress exhibits erratic behavior, indicating incipient divergence.
Keywords: similarity solution, stagnation-point flow, unsteadiness, oscillation, blowing.

السلوك الحرج لأقصى إجهاد قص داخل الطبقة الحدودية عند نقطة الركود غير مستقرة في وجود نفخ جداري ترددي

علي محمد بالحاج[1]
معهد العالي للعلوم والتقنية، الزهراء ، ليبيا
Ali.belhag@yahoo.com

هويدا مفتاح الشريف[2]
كلية تقنية الطيران المدني والارصاد الجوية، اسبيعة، ليبيا
hwedasharif@gmail.com

سليم علي الشاوش [3]
كلية تقنية الطيران المدني والارصاد الجوية، اسبيعة، ليبيا
alshaweshsalim2@gmail.com

المقدمة

تبحث هذه الورقة في تأثير عدم استقرار الجريان على أقصى إجهاد قص في الطبقة المتاخمة عند نقطة الركود غير المستقرة مع وجود النفخ عند الجدار. يعتمد التحليل على جريان لزج غير قابل للانضغاط ثنائي الأبعاد يقترب من صفيحة مستوية رأسية، وذلك وفق صياغة (Blyth و .Hall) . تم أخذ سرعة الجريان الحر المتغيرة دورياً مع الزمن، وكذلك النفخ المتذبذب عند الجدار، بعين الاعتبار.

http://www.doi.org/10.62341/jfhc2358

ومن خلال توظيف تحولات التشابه، تم اختزال معادلات نافير–ستوكس غير المستقرة الحاكمة إلى معادلة تشابه غير خطية تصف جريان الطبقة المتاخمة. وقد حُلَّت المعادلات الناتجة عددياً باستخدام مخطط الفروق المحدودة الضمني الكامل. جرى توصيف إجهاد القص عند الجدار من خلال المشتقة الثانية لدالة التشابه، وتم تتبع قيمته العظمى مع الزمن.

أظهرت النتائج أن أقصى إجهاد قص يزداد بزيادة معامل النفخ، في حين يتناقص مع ازدياد معامل عدم الاستقرار. ولكل مجموعة من معاملات الجريان، يبلغ إجهاد القص قيمة عظمى عند تردد اهتزازي محدد قبل أن يتجه نحو سلوك تقاربي.

إضافة إلى ذلك، يؤدي ازدياد عدم الاستقرار إلى تأخير حدوث أقصى إجهاد قص وتخفيف شدته، مع ملاحظة حدوث تباعد في قيمه عند نطاقات معينة من المعاملات. توفر هذه النتائج فهماً جديداً لجريان نقطة الركود غير المستقر مع النفخ عند الجدار.

الكلمات المفتاحية :حل التشابه، جريان نقطة الركود، عدم الاستقرار، الاهتزاز، النفخ.

Introduction

Stagnation points arise in numerous engineering and industrial applications, including aerodynamic heating of blunt bodies, vehicle flow management, cooling systems, surface coating, and mass transfer processes. At a stagnation point, the fluid velocity reduces to zero at the surface, forming a viscous boundary layer where wall shear stress— the tangential force exerted by the fluid—plays a critical role. Accurate prediction of this stress is essential, as it directly affects drag, surface erosion, and thermal performance.

The foundational study of stagnation-point boundary layers dates back to Hiemenz [1], who first solved the steady two-dimensional flow near a flat plate. Howarth later extended this work by incorporating viscous effects more rigorously [2]. A pivotal advancement came with Blyth and Hall's model of unsteady stagnation-point flow, which has since become a standard

http://www.doi.org/10.62341/jfhc2358

framework for analytical and numerical investigations of time-dependent impinging flows.

Building on this foundation, recent studies have explored increasingly complex scenarios. For instance, Khashi'ie et al. [3]examined unsteady separated stagnation-point flows in hybrid ferrofluids under magnetic fields and internal heat generation. The same authors also investigated suction and nanofluid effects on momentum and heat transfer over moving plates [4]. Roșca et al.[5] conducted numerical analyses of unsteady mixed convection at stagnation points, incorporating slip and nanofluid characteristics. Nasir et al. [6] addressed magnetohydrodynamic flows over Riga plates, combining electromagnetic and electrohydrodynamic influences. While these works provide valuable insights into velocity profiles, heat transfer, and skin friction, they offer limited analysis of the maximum shear stress within the unsteady boundary layer particularly its temporal evolution, dependence on flow unsteadiness, and response to wall oscillations.

Despite significant progress, most existing research focuses on mean flow properties, surface friction, or thermal behavior, with little attention to how peak shear stress varies in time. Specifically, the interplay between flow unsteadiness, oscillatory wall blowing/suction, and the resulting magnitude, timing, and frequency of maximum shear stress remains poorly understood. Moreover, the conditions under which this stress may amplify, destabilize, or diverge are not well characterized .

This study addresses these gaps by analyzing an unsteady two-dimensional stagnation-point flow based on the framework of Blyth and Hall [7], with time-periodic wall blowing or suction. Using similarity transformations, the unsteady Navier–Stokes equations are reduced to a single nonlinear ordinary differential equation governing the boundary layer. This equation is solved numerically

http://www.doi.org/10.62341/jfhc2358

via a fully implicit finite-difference scheme; a robust and widely validated method. The primary contribution lies in a systematic investigation of how the unsteadiness parameter, oscillation frequency, and blowing intensity jointly influence the peak wall shear stress. We identify critical regimes where the stress exhibits pronounced amplification, delayed onset, or signs of divergence, thereby offering new insights into the dynamic behavior of unsteady boundary layers under active wall control.

Similarity transformation and Numerical solution.

Similarity transformations.

The problem under consideration is that of two-dimensional version of Blyth and Hall [8], flow approaching a vertical flat plate. Referring to a set of Cartesian axes (x, y), the flat plate occupies $-\infty < x < \infty,\ y = 0$.

The velocity components are expressed as $u(x, y, t),\ v(x, y, t)$ in the x, y directions, respectively; governing equations, which describe the fluid motion, in this case are the two-dimensional unsteady Navier-Stokes equations.

In some simplified cases, such as a fluid travels through a rigid body (e.g, missile, sports ball, automobile, spaceflight vehicle), or in oil recovery industry crude oil that can be extracted from an oil field is achieved by gas injection, or equivalently, an external flow impinges on a stationary point called stagnation-point that is on the surface of a submerged body in a flow, of which the velocity at the surface of the submerged object is zero.

A stagnation point flow develops and the streamline is perpendicular to the surface of the rigid body. The flow in the vicinity of this stagnation point is characterized by Navier-Stokes equations. By introducing coordinate variable transformation, the number of independent variables is reduced by one or more. The governing equations can be simplified to the non-linear ordinary differential equations and are analytic solvable.

http://www.doi.org/10.62341/jfhc2358

Navier-Stokes Equations.

The full Navier-Stokes equations are difficult or impossible to obtain an exact solution in almost every real situation because of the analytic difficulties associated with the non-linearity due to convective acceleration. The existence of exact solutions are fundamental not only in their own right as solutions of particular flows, but also are agreeable in accuracy checks for numerical solutions.

The Navier-Stokes equations are a system of non-linear, coupled partial differential equations (PDEs) which are derived from the principles of mass and momentum conservation.

The equation of mass conservation, or continuity equation, can be written as:

$$u_x + v_y = 0 \tag{1}$$

The equations of momentum conservation for a fluid are obtained from the application of the force-momentum principle, and can be written:

x- momentum :

$$u_t + uu_x + vu_y = -\frac{1}{\rho}P_x + \upsilon\left[u_{xx} + u_{yy}\right] \tag{2}$$

y- momentum :

$$v_t + uv_x + vv_y = -\frac{1}{\rho}P_y + \upsilon\left[v_{xx} + v_{yy}\right] \tag{3}$$

with the parameters, kinematic viscosity υ , pressure P and density ρ .

The boundary conditions are taken as:

$$\begin{aligned} u = 0, \quad v = v_0(t) \qquad & at \qquad y = 0 \\ u \to U_e(t) \qquad & at \qquad y \to \infty \end{aligned} \tag{4}$$

Where $u, \& v$ the velocity components of the flow through the boundary layer are, $v_0(t)$ is the velocity of blowing\suction through the wall, $U_e(t)$ is unsteady potential velocity component.

http://www.doi.org/10.62341/jfhc2358

Near the surface, because of the no slip condition not being satisfied, a similarity solution is employed. We defined dimensionless similarity variables as ξ, η since:

$$\xi = Ax \tag{5}$$

$$\eta = \sqrt{\frac{A}{\upsilon}} * y \tag{6}$$

Where, A is a constant related with the body geometry, where $A > 0$.

The velocity components u and v of the boundary-layer flow are assumed to have solutions of the following form:

$$u = \xi * f_{\eta}(\eta, t) \tag{7}$$

Then, the y-direction velocity component v of the potential flow is immediately determined from the continuity equation (1), by substituting the foregoing velocity components u and v.

$$v = -\sqrt{\upsilon A} f(\eta, t) \tag{8}$$

Consider the unsteady periodic motion of an incompressible viscous fluid in the vicinity of the stagnation point at $x = y = 0$ on a blunt body. The potential flow approaches the body in the negative y-direction, impinges on the surface normally at the stagnation point flows away radially in all directions along the surface, and is assumed to have unsteady velocity components:

$$U_e = \xi a(t) \tag{9}$$

Where $a(t)$ is an arbitrary time-dependent function, as a case study it was chosen $a(t)$ as:

$$a(t) = \frac{1}{1 + \frac{\alpha}{\omega} \sin \omega t}, \tag{10}$$

Where, α is a constant related to free stream acceleration and ω is the potential flow frequency.

When $\alpha = 0$, the problem reduces to the steady case, that means $U_e \to Ax$.

http://www.doi.org/10.62341/jfhc2358

Corresponding to α & A, we can define the unsteadiness parameter D as:

$$D = \alpha / A$$

The equations of motion (1 to 3) for the two-dimensional unsteady flow of incompressible viscous fluid in the vicinity of a forward stagnation point are reduced to two partial differential equations for a potential flow field chosen to vary periodically as a function of time, using the following procedure.

Consider a general form of chain rule, similarity equation describes the stream-wise flow in stagnation point flow boundary layer:

$$\left(\frac{1}{A}\right) f_{\eta,t} + \left(f_{\eta}\right)^2 - f\, f_{\eta\eta} = \left(\frac{1}{A}\right) a_t(t) + [a(t)]^2 + f_{\eta\eta\eta} \quad (11)$$

Initial and boundary conditions.

The boundary conditions in Eq.(11) in a generalized form and our assumptions were applied to achieve a special case which under the effect of flow parameters' changing.

For that, the boundary conditions are reformed according to our case study as:

$$f_{\eta}(0,\eta) = 0, \qquad f(0,t) = -\sqrt{\frac{1}{A\upsilon}}\, v_0(t),$$

$$\eta \to \infty, \qquad f_{\eta} \to a(t) \quad (12)$$

$v_0(t)$ was chosen as: $v_0(t) = \Delta \cos \omega t$ (13)

Where Δ is the amplitude of the oscillating flow due to blowing/suction at the wall, and ω is the oscillation frequency.

By substituting by Eq.(12) in Eq.(13), we get:

http://www.doi.org/10.62341/jfhc2358

$f(0,t) = -\sqrt{\frac{1}{A\upsilon}}\,\Delta\cos\omega t$, hence, $A.\upsilon, \Delta$ are constants, we can introduce, $k = -\sqrt{\frac{1}{A\upsilon}}\,\Delta$, and named it as "blowing parameter".

To solve equations (11) numerically, A fully implicit finite difference based PDE solver is used (Implicit Euler)

Results and Discussion.

Effect of Flow Parameters on wall shear stress τ_{wall}

According to our assumptions, $f_{\eta\eta}(\eta)$ is the similarity function refers to the shear stress distribution within the boundary layer, since:

$$\tau = \upsilon\frac{\partial u}{\partial y} = \upsilon\left(\frac{\partial u}{\partial \eta}\right)\left(\frac{\partial \eta}{\partial y}\right)$$

$$from\ our\ assumptions: \frac{\partial u}{\partial \eta} = A\,x\,f_{\eta}(\eta)\ \&\ \frac{\partial \eta}{\partial y} = \sqrt{\frac{A}{\upsilon}}$$

$$\therefore \tau \propto f_{\eta\eta}(\eta)$$

In the following sections we will discuss the results considering the influence of flow parameters on shear stress within the boundary layer.

Effect of blowing parameter on the wall shear stress.

The following table includes the maximum values of $f_{\eta\eta}(\eta)$ which was found within a period of time don't exceed 0.6 second from the beginning of the unsteady motion, in table (1) were included the time at which $f_{\eta\eta}(\eta)$ has a maximum value at ($D = 2,\ k = (10, 50, 100, 200)$. The maximum shear stress may be exist inside the viscous boundary layer if k & ω don't exceed specific values. But for higher values maximum shear stress exist at the wall (at $\eta \approx 0$).

http://www.doi.org/10.62341/jfhc2358

These values were searched to correspond the value of $D = 2$, and various values of k & ω. These values were plotted in figure (1).

Associating to figure (1), it could to be commented the following:

- Maximum $f_{\eta\eta}(\eta)$ increases with blowing parameter k.
- For each k value, $f_{\eta\eta}(\eta)$ increases rapidly to its maximum value, corresponds to a specific value of the oscillation parameter at $\omega = \varTheta$ where $\varTheta$ within the range of $[30 - 70] 1/s$. $f_{\eta\eta}(\eta)$ decreases during the range $\varTheta \approx [70 - 300]\ 1/s$, to go almost constantly after $\omega \geq 300\ \ 1/s$.

TABLE 1. $f_{\eta\eta} - profile$ maximum values indicates maximum shear stress $f_{\eta\eta}(\eta)_{max.}$ vs. oscillation frequency ω at different values of blowing parameter K at unsteadiness parameter D= 2

ω $(1/s)$	$f_{\eta\eta}(\eta)_{max.}\ at\ D = 2$, within 0.6 s			
	(k=200)	(k=100)	(k=50)	(k=10)
1	9.258861	7.299397	8.337737	
5	14.12924	12.33942	10.30847	4.717446
10	15.61116	14.06375	11.86223	5.029949
20	16.77482	15.15149	12.77014	4.470926
30	17.20849	15.50646	12.72162	3.952873
40	17.41046	15.59892	12.29333	3.577264
70	17.42147	14.83062	10.56896	2.859268
100	16.72094	13.42369	8.950562	2.508152
200	13.28164	9.575809	5.944116	1.977901
300	7.475956	5.844906	4.210639	1.726169
400	7.604838	5.611407	3.692614	1.57697
500	7.696629	5.881554	4.027748	1.657984

http://www.doi.org/10.62341/jfhc2358

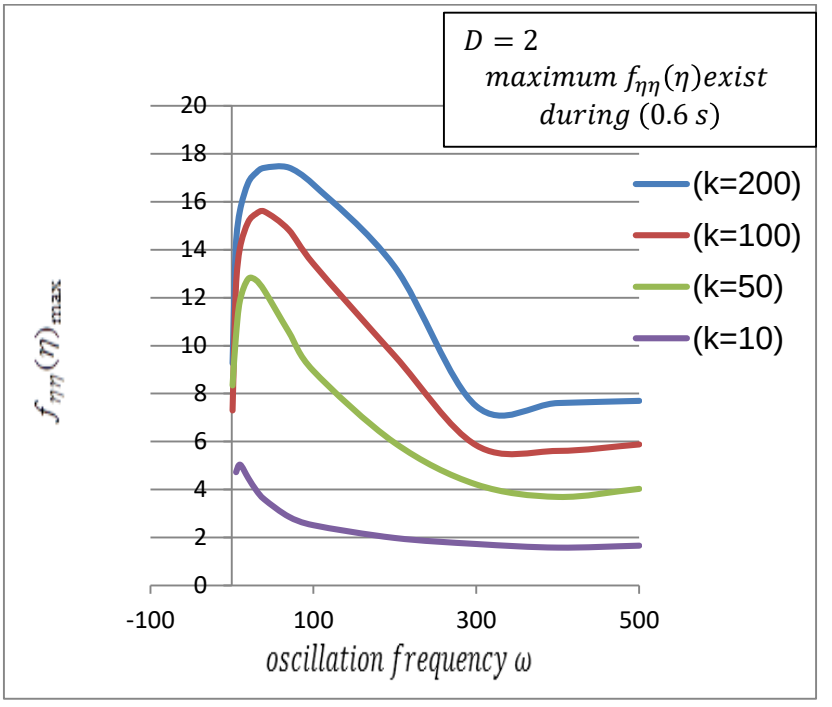

Fig. 1: $f_{\eta\eta} - profile$ maximum values indicates maximum shear stress $f_{\eta\eta}(\eta)_{max.}$ vs. oscillation frequency ω at different values of *blowing parameter* k at *unsteadiness parameter* $D = 2$

Effect of unsteadiness parameter on the shear stress.

In the previous section, the effect of the blowing parameter on the shear stress was discussed, in this section we'll discuss the effect of the unsteadiness parameter on $f_{\eta\eta}(\eta)_{max.}$, at $k = 100$.

Associating to table (1) and figure (1), it could to be commented the following:

- Maximum $f_{\eta\eta}(\eta)$ decreases with the increasing of the unsteadiness parameter D .

http://www.doi.org/10.62341/jfhc2358

- For each D, $f_{\eta\eta}(\eta)$ increases rapidly to its maximum value, corresponds to a specific value of the oscillation parameter at $\omega = \varpi$ where ϖ within the range of $[30-40]1/s$.
- $f_{\eta\eta}(\eta)$ decreases during the range of $\varpi \approx [40-300]\ 1/s$, to goes almost constantly after $\omega \geq 300\ \ 1/s$.
- $f_{\eta\eta}(\eta)_{max.}$ is almost the same in the range of $\omega \approx [100-300]\ 1/s$, so the effect of D is absent.
- As shown in table (2), at values of $D \geq 8$, corresponding the values of $\omega \leq 10\ \ 1/s$, $f_{\eta\eta}(\eta)_{max.} \longrightarrow \infty$.

TABLE 2: $f_{\eta\eta} - profile$ maximum values indicates maximum shear stress $f_{\eta\eta}(\eta)_{max.}$ vs. oscillation frequency ω, $blowing\ parameter\ k = 100$ at different values of $unsteadiness\ parameter\ D$

ω $(1/s)$	$f_{\eta\eta}(\eta)_{max.}\ at\ k = 100$					
	D = 0.5	D = 2	D = 4	D = 6	D = 8	D = 10
1	11.57255	7.299397	5.174363	3.967744	diverge	diverge
5	15.14843	12.33942	10.58405	9.544457	diverge	diverge
10	15.86737	14.06375	12.62341	11.73697	11.10935	diverge
20	16.20153	15.15149	14.16732	13.50914	13.01286	12.66048
30	16.2220	15.50646	14.80039	14.23102	13.83276	13.44041
40	16.02257	15.59892	15.04938	14.63641	14.37666	14.11536
70	14.951	14.83062	14.66735	14.50092	14.33132	14.15852
100	13.4547	13.42369	13.38082	13.33619	13.28975	13.24147
200	9.537017	9.575809	9.629546	9.68594	9.745383	9.808267
300	5.97941	5.844906	5.677917	5.540308	5.389138	5.287292
400	5.830675	5.611407	5.317554	5.021995	4.72474	4.425796
500	6.104455	5.881554	5.584054	5.286202	4.98799	4.689408

http://www.doi.org/10.62341/jfhc2358

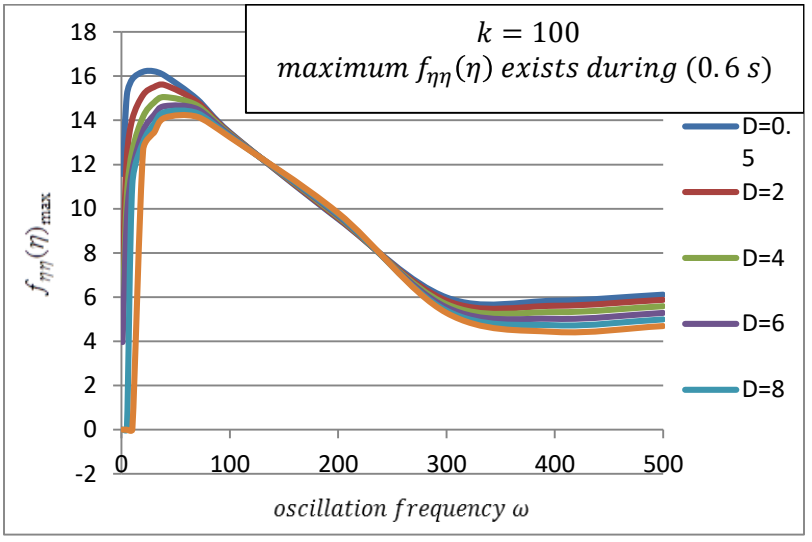

Fig.2 : $f_{\eta\eta} - profile$ maximum values indicates maximum shear stress $f_{\eta\eta}(\eta)_{max.}$ vs. oscillation frequency ω, $blowing\ parameter\ k = 100$ at different values of $unsteadiness\ parameter\ D$

The observation of the time of maximum shear stress.

It was interesting to determine the time at which $f_{\eta\eta}(\eta)_{max.}$ occurs, this critical time changes according to flow parameters changing, so table (3) and figure (3) are valid only for the corresponding flow parameters' values.

It was selected for $k = 100$, the unsteadiness parameter values as : $(D = 0.5, 2, 6, 10)$and $\omega\ (from\ 5\ to\ 700\ \frac{1}{s})$.

By analyzing the data installed in table (3), it could be comment that:

- The time at which $f_{\eta\eta}(\eta)_{max.}$ exists, occurs earlier if D was smaller.
- As the oscillation frequency becomes higher, $f_{\eta\eta}(\eta)_{max.}$ occurs earlier.
- For the considered range of ω values, the maximum time that $f_{\eta\eta}(\eta)$ can take to reach its highest value is $t = 0.6s$ at

http://www.doi.org/10.62341/jfhc2358

$\omega = 5\ \frac{1}{s}, D = 2, k = 100$. Table (3) shows the time at which the previous results were illustrated in figure (3).

TABLE 3. $f_{\eta\eta} - profile$ maximum value occurrence time vs. oscillation frequency ω, $blowing\ parameter\ k = 100$ at different values of $unsteadiness\ parameter\ D$

$oscillation\ frequency\ \omega$	$time\ [f_{\eta\eta}(\eta)_{max.}] at\ k = 100$			
	D=0.5	D=2	D=6	D=10
5	0.35	0.5	0.57	0.6
10	0.19	0.19	0.28	0.3
20	0.1	0.12	0.14	0.15
30	0.08	0.08	0.08	0.1
40	0.07	0.07	0.08	0.08
60	0.05	0.06	0.06	0.06
80	0.05	0.05	0.05	0.05
90	0.04	0.04	0.04	0.04
100	0.04	0.04	0.04	0.04
104	0.04	0.04	0.04	0.04
110	0.04	0.04	0.04	0.04
120	0.04	0.04	0.04	0.04
140	0.03	0.03	0.03	0.03
160	0.03	0.03	0.03	0.03
200	0.03	0.03	0.03	0.03

http://www.doi.org/10.62341/jfhc2358

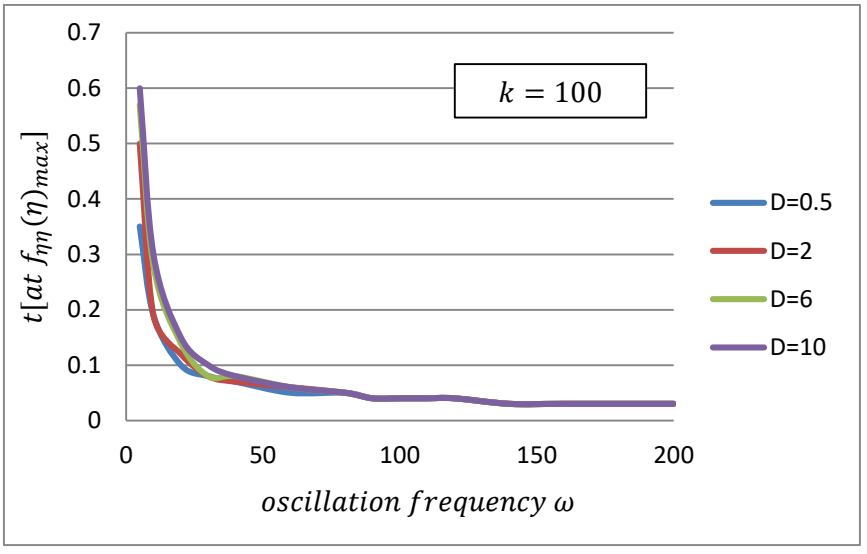

Fig.3: The time at which $f_{\eta\eta} - profile$ maximum value occurs vs. oscillation frequency ω, $blowing\ parameter\ k = 100$ at different values of $unsteadiness\ parameter\ D$

The results align well with established principles of unsteady stagnation-point flows and time-dependent boundary layer dynamics. A pronounced peak in wall shear stress occurs at intermediate oscillation frequencies (approximately 30–70 rad/s). This peak arises from a near-resonant interaction between the imposed wall oscillation period and the viscous response time of the near-wall fluid. At these frequencies, the oscillatory momentum from wall blowing penetrates deeply into the boundary layer, amplifying the stream-wise velocity gradient near the wall and thereby maximizing shear stress. This behavior is consistent with Stokes' second problem, where peak shear stress occurs when the oscillation frequency yields an optimal Stokes layer thickness [8, 9].

At higher frequencies ($\omega \gtrsim 200$ rad/s), the Stokes layer becomes extremely thin, confining oscillations to a narrow region adjacent to the wall. Viscous effects dominate in this regime, introducing a

http://www.doi.org/10.62341/jfhc2358

significant phase lag between wall motion and fluid response. Consequently, less oscillatory momentum is transmitted into the boundary layer, causing wall shear stress to decline and eventually plateau, a trend widely documented in high-frequency oscillatory viscous flows[10, 11].

Increasing the blowing parameter K leads to a steady, monotonic rise in wall shear stress. Physically, K represents a source of momentum normal to the wall; greater blowing injects more fluid vertically, intensifying the streamwise velocity gradient at the surface. This mechanism is well known in laminar boundary layer studies: wall injection enhances near-wall velocity gradients, thereby increasing shear stress. Similar observations have been reported by Zaturska et al. [12] and Al-Sanea & El-Amin [13].

The influence of the unsteadiness parameter D is nonlinear, as expected. For small to moderate values ($D \lesssim 1$), increasing D strengthens the unsteady acceleration in the free stream, enhancing flow deformation near the wall and raising shear stress. However, for larger D, the phase relationship between the outer flow and wall oscillations shifts, leading to boundary layer thickening. This reduces the near-wall velocity gradient and causes shear stress to decrease. This non-monotonic response agrees with earlier analyses of unsteady stagnation-point flows [14, 15], and is additionally influenced in the present study by the phase-coupled effect of oscillatory wall blowing.

Overall, the observed trends-the peak-and-decay response with respect to ω, the monotonic increase with K, and the non-monotonic variation with D - are fully consistent with theoretical expectations for unsteady viscous flows subject to periodic wall conditions and time-varying free-stream forcing.

Conclusion

This study shows that, in unsteady stagnation-point flows with wall blowing, the maximum wall shear stress is strongly governed by two

http://www.doi.org/10.62341/jfhc2358

non-dimensional parameters: the blowing intensity and the flow unsteadiness. Increasing the blowing parameter consistently elevates peak shear stress, whereas higher unsteadiness generally suppresses it. A critical amplification of shear stress occurs at intermediate oscillation frequencies, where resonant-like interaction between wall forcing and viscous response is most effective.

The timing of the peak shear stress is also sensitive to both parameters: it occurs earlier at higher oscillation frequencies and under lower unsteadiness. Importantly, the analysis identifies critical regimes-particularly at specific combinations of frequency, blowing, and unsteadiness-where shear stress exhibits extreme magnification or signs of divergence. These findings provide valuable guidance for applications involving flow control, surface loading mitigation, and thermal management near stagnation regions.

Overall, the results underscore the necessity of jointly accounting for unsteadiness and active wall forcing in the design and optimization of engineering systems featuring stagnation-point flows, such as in aerospace thermal protection, turbine cooling, and aerodynamic control surfaces.

References

[1]. K. Hiemenz, Die Grenzschicht an einem in den gleichförmigen Flüssigkeitsstrom eingetauchten geraden Kreiszylinder, Dinglers Polytech. J. 326 (1911) 321–324.

[2]. L. Howarth, On the solution of the boundary-layer equations, Proc. R. Soc. A 164 (1938) 547–579.

[3]. M. Khashi'ie, N. M. Arifin, I. Pop, Unsteady separated stagnation-point flows with magnetic fields and heat generation in hybrid ferrofluids, Int. J. Heat Mass Transf. 182 (2022) 122135.

[4]. M. Khashi'ie, N. M. Arifin, I. Pop, Effects of suction and nanofluid transport on momentum and heat transfer in moving plate configurations, Appl. Therm. Eng. 220 (2024) 119876.

http://www.doi.org/10.62341/jfhc2358

[5]. D. Roșca, A. V. Roșca, I. Pop, Numerical analysis of unsteady mixed convection stagnation-point flows with slip or nanofluid effects, Comput. Fluids 254 (2023) 105812.

[6]. S. Nasir, Z. Shah, E. Alaidarous, Magnetohydrodynamic stagnation flows over electro-magnetohydrodynamic Riga plates, J. Magn. Magn. Mater. 580 (2023) 169872.

[7]. M. G. Blyth, P. Hall, Oscillatory flow near a stagnation point, SIAM J. Appl. Math. 63 (5) (2003) 1604–1614.

[8]. J. T. Stuart, Double boundary layers in oscillatory viscous flow, J. Fluid Mech. 29 (1967) 1–16.

[9]. H. Schlichting, K. Gersten, Boundary-Layer Theory, 9th ed., Springer, Berlin, 2017.

[10]. N. Riley, Steady streaming, Annu. Rev. Fluid Mech. 33 (2001) 43–65.

[11]. X. Liu, L. Zheng, Oscillatory Stokes-layer characteristics at high frequency, Alexandria Eng. J. 61 (2022) 10235–10244.

[12]. M. B. Zaturska, W. H. H. Banks, P. G. Drazin, Oscillatory flows with suction and injection, J. Fluid Mech. 204 (1989) 375–393.

[13]. S. A. Al-Sanea, M. F. El-Amin, Effects of wall blowing and suction on laminar boundary-layer characteristics, Int. J. Heat Mass Transf. 172 (2021) 121087.

[14]. T. R. Mahapatra, S. K. Nandy, Unsteady stagnation-point flow and heat transfer over a stretching surface, Commun. Nonlinear Sci. Numer. Simul. 16 (2011) 374–388.

[15]. H. Xu, S. Liao, Analytical solutions of unsteady stagnation flows using homotopy analysis, Appl. Math. Comput. 266 (2015) 553–563.